Two 14-3-3 Binding Motifs Are Required for Stable Association of Forkhead Transcription Factor FOXO4 with 14-3-3 Proteins and Inhibition of DNA Binding

Tomas Obsil,[‡] Rodolfo Ghirlando, D. Eric Anderson,[§] Alison Burgess Hickman, and Fred Dyda*

Laboratory of Molecular Biology, National Institute of Diabetes, Digestive and Kidney Diseases, National Institutes of Health, 5 Center Drive, MSC 0560, Bethesda, Maryland 20892

Received July 18, 2003; Revised Manuscript Received September 30, 2003

ABSTRACT: The 14-3-3 proteins, a family of dimeric regulatory proteins, are involved in many biologically important processes. The common feature of 14-3-3 proteins is their ability to bind to other proteins in a phosphorylation-dependent manner. Through these binding interactions, 14-3-3 proteins work as molecular scaffolds, modulating the biological functions of their partners. 14-3-3 proteins recognize short motifs containing a phosphorylated serine or threonine residue. In this study, we have quantitatively characterized the in vitro interactions among 14-3-3, the Forkhead transcription factor FOXO4, and its target DNA, the insulin response element. Phosphorylation of FOXO4 (residues 11−213) by protein kinase B at Thr-28 and Ser-193 creates two 14-3-3 binding motifs. Analytical gel filtration and sedimentation equilibrium experiments indicate that doubly phosphorylated FOXO4 and 14-3-3ζ form a complex with 1:2 molar stoichiometry and a K_D of less than 30 nM. In contrast, singly phosphorylated FOXO4 mutants bind 14-3-3ζ with significantly lower affinity while retaining the ability to bind DNA. An active role for 14-3-3 in the disassembly of the FOXO4/DNA complex is demonstrated by the fact that, in the presence of 14-3-3, two phosphorylated 14-3-3 binding motifs are needed for the complete inhibition of FOXO4 binding to its target DNA.

The 14-3-3 proteins, a highly conserved family of regulatory proteins, are involved in many biologically important processes, such as cell cycle control, apoptosis, and oncogenesis (*1*). Seven mammalian 14-3-3 isoforms encoded by seven distinct genes have been identified to date. The main feature of 14-3-3 proteins is their ability to bind to other proteins in a phosphorylation-dependent manner. In certain contexts, 14-3-3 proteins work as molecular scaffolds modulating the conformation of their binding partners; if the binding partner is an enzyme, this can affect the enzymatic properties of the binding partner (*2*, *3*). 14-3-3 proteins can also regulate the subcellular localization of their partners by masking or obscuring a nearby targeting sequence, such as a nuclear localization sequence (NLS)[1] or a nuclear export sequence (NES) (*4*). Proteins shown to be subject to such regulation include CDC25 phosphatases (*5*), telomerase (*6*), histone deacetylase (*7*), and FOXO transcription factors (*8*−*10*).

14-3-3 proteins recognize a motif containing either a phosphorylated serine (pS) or a phosphorylated threonine (pT) residue, which is present in most known 14-3-3 binding partners (*1*, *11*, *12*). Two optimal 14-3-3 binding motifs, RSXpSXP and RXY/FXpSXP, have been identified using oriented peptide library screening approaches (*11*, *13*). All 14-3-3 isoforms form very stable homo- and heterodimers, and share very similar three-dimensional structure (*14*, *15*). Two monomers, each consisting of nine antiparallel α-helices, create a cup-shaped dimer with a large, wide (approximately 40 Å) central channel containing two amphipathic grooves on either side, facing toward the middle of the channel. Several crystal structures of 14-3-3 complexes with short phosphopeptides representing optimal binding motifs have been determined (*11*, *15*). In all cases, the phosphopeptides are bound within the two amphipathic grooves of the central channel.

Many binding partners of 14-3-3 proteins contain multiple phosphorylation sites embedded in 14-3-3 recognition motifs (*16*). An intriguing example of the critical role of multiple 14-3-3 binding motifs within a single protein molecule is provided by the FOXO subfamily of Forkhead transcription factors. Four mammalian FOXO factors, FOXO1 (FKHR), FOXO3a (FKHR-L1), FOXO4 (AFX), and FOXO6 have been identified to date. FOXO transcription factors participate in a number of important biochemical pathways including cell cycle regulation, cell death, and the control of cell metabolism (*17*). For example, FOXO4 is involved in cell cycle regulation and the process of tumor initiation and progression (*18*, *19*). A *Caenorhabditis elegans* FOXO protein, desig-

* To whom correspondence should be addressed: Phone: (301) 402-4496. Fax: (301) 496-0201. E-mail: dyda@ulti.niddk.nih.gov.

[‡] Current address: Department of Physical and Macromolecular Chemistry, Faculty of Science, Charles University, Hlavova 2030/8, 12843 Prague 2, Czech Republic.

[§] Current address: Laboratory of Bioorganic Chemistry, National Institute of Diabetes, Digestive and Kidney Diseases, National Institutes of Health.

[1] Abbreviations: IGF, insulin-like growth factor; PKB, protein kinase B; PKA, protein kinase A; PI3K, phosphatidylinositol 3-kinase; IRE, insulin response element; GST; glutathione S-transferase; PAGE, polyacrylamide gel electrophoresis; WT, wild type; NLS, nuclear localization sequence; NES, nuclear export sequence; CK1, casein kinase 1.

10.1021/bi0352724
Published on Web 12/02/2003

A

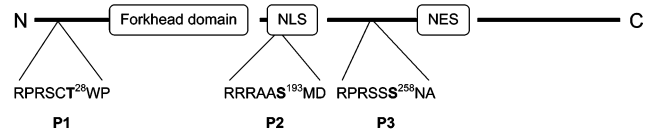

B

	P1	P2	P3
FOXO1 (FKHR)	RPRSCT^{24}WP	RRRAAS^{256}MD	RPRTSS^{319}NA
FOXO3a (FKHR-L1)	RPRSCT^{32}WP	RRRAVS^{253}MD	RSRTNS^{315}NA
FOXO4 (AFX)	RPRSCT^{28}WP	RRRAAS^{193}MD	RPRSSS^{258}NA
FOXO6	RPRSCT^{26}WP	RRRAVS^{184}MD	-
DAF-16	RDRSNT^{54}WP	RTRERS^{240}NT^{242}	RPRTQS^{314}NL

FIGURE 1: Diagram of the FOXO4 primary structure. (A) The positions of PKB phosphorylation sites P1, P2, and P3 are indicated by their sequence. NLS = nuclear localization sequence; NES = nuclear export sequence. (B) Sequence comparison of PKB phosphorylation sites of human FOXO1, FOXO3a, and FOXO4, mouse FOXO6 transcription factors, and their *C. elegans* homologue DAF-16. Numbered serine (S) and threonine (T) residues (in bold) have been shown to be phosphorylated. Note that the P3 site is not present in FOXO6.

nated DAF-16, has also been identified (*20*). Forkhead transcription factors exert their effects by binding to a DNA sequence containing a core consensus recognition motif, 5′-(A/C)AA(C/T)A-3′.

A current model for the regulation of FOXO proteins suggests that FOXO transcription factors can shuttle continuously between the nucleus and the cytoplasm. In the absence of protein kinase B (PKB) activity, FOXO proteins are predominantly located in the nucleus and the rate of import exceeds the rate of export. This shift toward nuclear localization is presumably the result of DNA binding by FOXO proteins. After PKB activation by the phosphatidylinositol 3-kinase (PI3K) signaling pathway, PKB phosphorylates FOXO on multiple sites, and induces binding to 14-3-3 proteins which are present within the nucleus. This association is believed to cause the release of the FOXO proteins from the DNA. PKB-mediated phosphorylation of FOXO proteins is followed by phosphorylation of additional sites by CK1 and rapid export of FOXO proteins from the nucleus. Once in the cytoplasm, FOXO proteins remain phosphorylated and bound to 14-3-3, thereby preventing nuclear reimport, likely the result of masking a FOXO nuclear localization sequence by bound 14-3-3. The net result is a shift in the equilibrium of FOXO localization toward the cytoplasm (*9*, *10*, *17*, *21*−*25*).

It has been demonstrated both in vitro and in vivo that FOXO1, FOXO3a, and FOXO4 are phosphorylated by PKB on several residues (Figure 1). For FOXO1, these were shown to be Thr-24 (site P1), Ser-256 (site P2), and Ser-319 (site P3), and phosphorylation results in the binding to 14-3-3 (*8*). FOXO3a is phosphorylated by PKB at equivalent residues as FOXO1 (*8*). Although the equivalent residues in FOXO4 can also be phosphorylated by PKB, the relevance of phosphoryation at the P1 site is not yet clear (*8*, *17*, *24*, *26*). PKB phosphorylates substrates that carry an RXRXXS/T motif, which is close to the consensus 14-3-3 binding motif (*1*).

Two of the sites, P1 and P2, border the functional DNA binding domain of the transcription factor (*27*), raising the possibility that the two sites could anchor the DNA binding domain in the central channel of the 14-3-3 dimer, thereby masking the DNA binding surface and inhibiting DNA binding. To investigate the roles of phosphorylation and complex formation with 14-3-3 in the DNA binding activity of FOXO proteins, we have chosen a quantitative in vitro approach using recombinant proteins expressed in *Escherichia coli*. Our results using sedimentation equilibrium indicate that phosphorylation of FOXO4 by PKB on Thr-28 (site P1) and Ser-193 (site P2) leads to a tight association of FOXO4 with 14-3-3ζ, causing complete inhibition of DNA binding, most likely caused by the masking of the DNA binding surface of the Forkhead domain by 14-3-3. In contrast, singly phosphorylated FOXO4 point mutants bind 14-3-3ζ with approximately the same affinity as they bind DNA, providing an elegant quantitative explanation for the requirement for multiple 14-3-3 binding motifs to effect biological function.

MATERIALS AND METHODS

Expression and Purification of FOXO4. DNA encoding human $FOXO4_{11-213}$ was generated by PCR amplification using full-length FOXO4 cDNA (*23*; a gift of Dr. A. M. Brownawell) and ligated into pGEX-4T-1 (Amersham Pharmacia Biotech) using the *Bam*HI and *Xho*I sites. The entire coding region was sequenced to confirm that no mutations had been introduced. Since FOXO4 contains a cryptic thrombin cleavage site, the thrombin cleavage site of the pGEX plasmid was mutated to a TEV cleavage site using the QuikChange mutagenesis kit (Stratagene). Point mutants of FOXO4 were similarly generated. $FOXO4_{11-213}$ (WT or mutants) was expressed as a glutathione S-transferase (GST) fusion protein by IPTG induction for 12 h at 20 °C and purified from *E. coli* BL21(DE3) using Glutathione Sepharose 4B according to the manufacturer's instructions (Amersham Pharmacia Biotech). The GST tag was removed by incubation for 1 h at 30 °C with 250 U of TEV protease (specific activity 10 U/1 μg)/mg of protein. After cleavage, $FOXO4_{11-213}$ was purified using cation-exchange chromatography on a HS/M 4.6 × 100 column (PerSeptive Biosystems). Protein was eluted using a 50−700 mM NaCl gradient in 50 mM sodium citrate (pH 6.3), 1 mM DTT, and 1 mM EDTA, and dialyzed overnight against buffer 1 (20 mM Tris [pH 7.5], 100 mM NaCl, 1 mM EDTA, 1 mM DTT).

Phosphorylation of FOXO4. Purified $FOXO4_{11-213}$ in buffer 1 was phosphorylated by incubation for 2 h at 30 °C with 9 U of PKBα (Upstate Biotechnology)/mg of protein in the presence of 10 mM magnesium acetate and 0.2 mM ATP. After phosphorylation, $FOXO4_{11-213}$ was repurified using cation-exchange chromatography as described above. Eluted protein was dialyzed against buffer 2 (20 mM Tris [pH 7.5], 100 mM NaCl, 1 mM EDTA, 2 mM DTT, 10% [w/v] glycerol).

Expression and Purification of 14-3-3. 14-3-3ζ was expressed and purified as described previously (*3*). Briefly, 14-3-3ζ was expressed as a histidine-tagged protein by IPTG induction for 12 h at 20 °C, and purified from *E. coli* BL21-(DE3) using Chelating Sepharose. The histidine tag was removed by incubation for 6 h at 15 °C with 10 U of thrombin/mg of protein. After cleavage, 14-3-3ζ was purified using anion-exchange chromatography on an HQ/M 4.6 ×

100 column (PerSeptive Biosystems). The protein was eluted using a 50−600 mM NaCl gradient in 50 mM Tris−HCl (pH 8.0) and 1 mM DTT, and dialyzed overnight against buffer 3 (20 mM Tris [pH 7.5], 100 mM NaCl, 1 mM EDTA, 5 mM DTT, 10% [w/v] glycerol).

Analytical Gel Filtration. Analytical gel filtration experiments to monitor complex formation among $FOXO4_{11-213}$, 14-3-3ζ, and DNA were performed on a Pharmacia SmartSystem Superdex 75 column in buffer 1 equilibrated at 4 °C. Typical samples (50 μL) contained 30 μM $FOXO4_{11-213}$ (WT or mutants), 30 μM DNA (see below), and 60 μM 14-3-3ζ in buffer 1. Oligonucleotides representing half of the insulin response element (designated hIRE; sequence 5′-GCAAAACAAA-3′ and its reverse complement) were synthesized on a 1 μmol scale, and purified using a 20% acrylamide/7 M urea TBE gel. After electroelution and desalting on a C18-Sepac column (Waters), oligonucleotides were resuspended in 20 mM Tris (pH 7.5) and 1 mM EDTA, mixed in an equimolar ratio, and annealed by heating to 70 °C for 10 min followed by slow cooling. Fractions from gel filtration (50 μL each) were analyzed using 4−12% NuPAGE gels (Invitrogen).

Analytical Ultracentrifugation. Sedimentation equilibrium experiments were performed using a Beckman XL-A analytical ultracentrifuge as previously described (*3*, *28*). Sedimentation equilibrium experiments of the phosphorylated $FOXO4_{11-213}$:14-3-3ζ complexes were conducted at loading concentrations of 10−17 μM, and data were collected at 280 nm. Experiments to determine the stoichiometry of the $FOXO4_{11-213}$:hIRE complexes were carried out at loading concentrations of 17−20 μM (λ = 292 nm), whereas experiments to estimate the binding affinity of $FOXO4_{11-213}$ for hIRE were carried out at 1/10 these loading concentrations (λ = 260 nm). All experiments were carried out at 4.0 °C and rotor speeds ranging from 8000 to 16000 rpm. Samples were dialyzed against buffer 4 (20 mM Tris−HCl [pH 7.5], 100 mM NaCl, 1 mM EDTA, 2 mM 2-mercaptoethanol) prior to analysis.

Electrophoretic Mobility Shift Assay. Samples containing 0.7 nmol of $FOXO4_{11-213}$ (wild type or mutants) and 1.4 nmol of 14-3-3ζ were incubated with 0.7 nmol of hIRE for 30 min at 4 °C in a buffer containing 20 mM Tris (pH 7.5), 100 mM NaCl, 1 mM EDTA, and 2 mM DTT. Samples were resolved on native 4−20% TBE−PAGE, and gels were either silver stained for DNA visualization (*26*) or stained with Coomassie Blue.

Mass Spectroscopy Analysis. Samples for electrospray mass spectrometry were dialyzed against several changes of 2−5% acetic acid, then diluted with two parts of 2% acetic acid/40% methanol, and continuously infused (15 μL/min) into the conventional enclosed electrospray source of a Z-spray-equipped Quattro LC mass spectrometer (Micromass, Altrincham, U.K.) operated in the positive mode. Final analytical spectra were collected with analyzer settings "LM Res" and "HM Res" of 15.7 to allow for resolution of phosphorylation isoforms and truncation products. Due to the low sensitivity of the instrument in this mode, data accumulation per spectrum of 5−15 min for samples of 0.2−1 mg/mL was typical. When fine structures in masses of samples were indicated in the traditional, non-Bayesian, transformed spectra, these features were confirmed in the fine structure of the dominant multiply charged peaks from the original mass spectrum. Side-by-side spectra of hen lysozyme (Sigma) were obtained to verify nominal mass accuracy available during each set of measurements using the same instrument settings. No corrections to measured masses were made on the basis of these control experiments.

RESULTS

PKB Phosphorylates $FOXO4_{11-213}$ at Thr-28 and Ser-193. It has been demonstrated that PKB phosphorylates FOXO4 at Thr-28 (site P1), Ser-193 (site P2), and Ser-258 (*17*, *24*, *26*). However, among FOXO4's close homologues FOXO1 and FOXO3a, only phosphorylations at the P1 site and P1 + P2 sites (*8*, *23*), respectively, have been shown to be important for binding to 14-3-3. Recently, a new member of the FOXO subfamily has been described and designated as FOXO6 (*30*). This novel Forkhead transcription factor shows high overall homology to other FOXO members, but lacks the region containing the third PKB phosphorylation site (P3 site). We therefore elected to restrict our analysis to the N-terminal half of FOXO4, residues 11−213, which contains the Forkhead DNA binding domain flanked by two PKB phosphorylation/14-3-3 binding sites, P1 and P2 (Figure 1).

Recombinantly expressed $FOXO4_{11-213}$ was phosphorylated in vitro using PKB. To determine the stoichiometry and completeness of the phosphorylation reaction, we used electrospray mass spectrometry. For unphosphorylated $FOXO4_{11-213}$, we obtained a molecular mass of 22550.4 Da (calculated 22548.5 Da), whereas for PKB-phosphorylated $FOXO4_{11-213}$, the measured mass was 22711 Da (calculated 22708.5). The mass difference of 160.6 Da between the two species indicates that PKB phosphorylates $FOXO4_{11-213}$ at two sites. We did not detect any unphosphorylated or singly phosphorylated $FOXO4_{11-213}$ in the sample treated with PKB, indicating that the phosphorylation was complete within our detection abilities. To confirm that the phosphorylation sites were Thr-28 (site P1) and Ser-193 (site P2), these residues were individually mutated to alanine, and the analysis was repeated following incubation with PKB. The measured mass differences relative to fully phosphorylated $FOXO4_{11-213}$ (T28A, −106 Da; S193A, −92.2 Da) correspond closely to the calculated mass difference (T28A, −110 Da; S193A, −96 Da) for the two proteins assuming the sequence change and the loss of a single phosphorylation site.

Doubly Phosphorylated $FOXO4_{11-213}$ Binds 14-3-3 with Higher Affinity than Singly Phosphorylated $FOXO4_{11-213}$. Next, we tested whether phosphorylation of FOXO4's P1 and P2 sites created functional 14-3-3 binding motifs. We used both analytical gel filtration (Figure 2) and analytical ultracentrifugation (Table 1) to monitor the binding of doubly phosphorylated $FOXO4_{11-213}$ ($dpFOXO4_{11-213}$) to 14-3-3ζ. When unphosphorylated $FOXO4_{11-213}$ was mixed with twice the stoichiometric amount of 14-3-3ζ, the proteins eluted during gel filtration as two overlapping yet distinct peaks (Figure 2D). However, when $dpFOXO4_{11-213}$ was mixed with twice the stoichiometric amount of 14-3-3ζ, all the protein eluted as a single peak (Figure 2C). Thus, phosphorylation of P1 + P2 sites by PKB is necessary for the stable association of FOXO4 with 14-3-3 proteins.

The stoichiometry of the $dpFOXO4_{11-213}$:14-3-3ζ complex was determined by sedimentation equilibrium measurements; this gave a buoyant mass of the monodisperse complex of

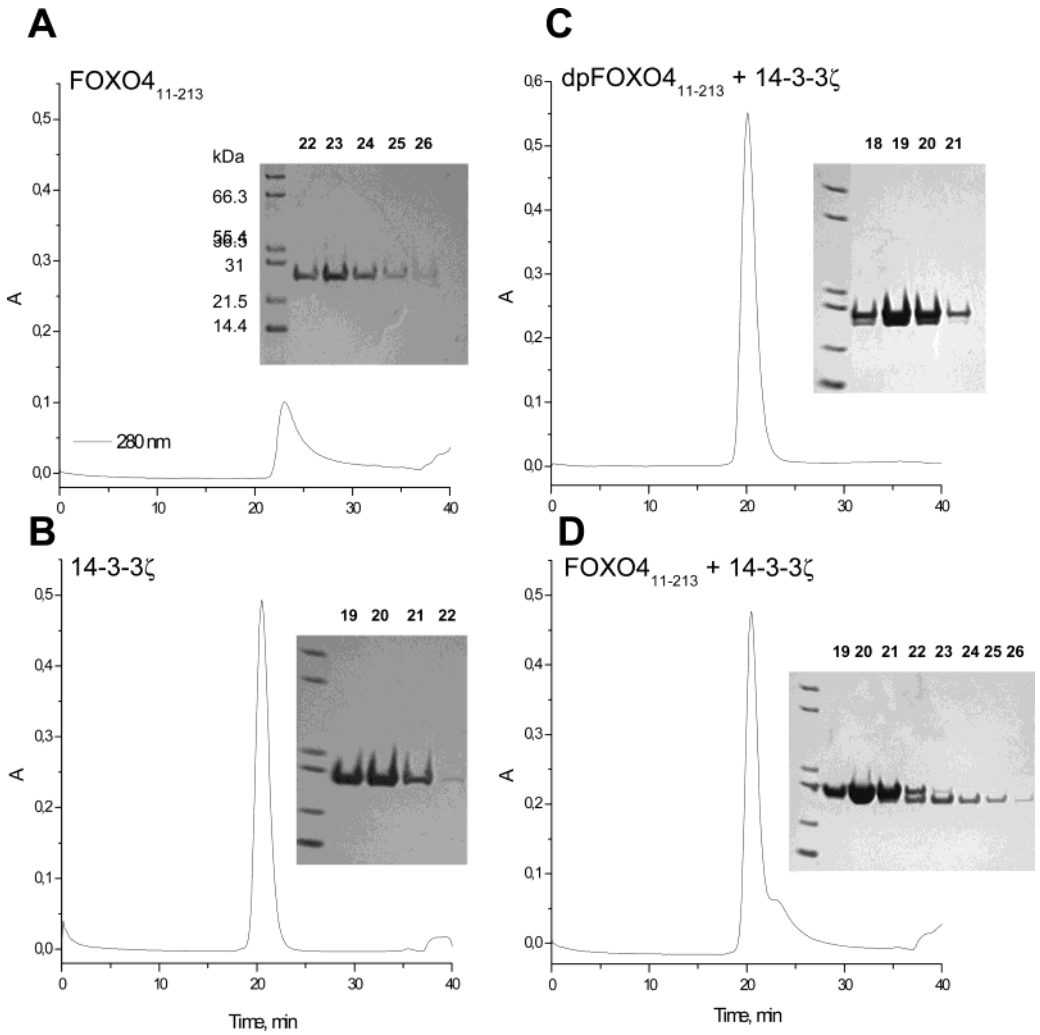

FIGURE 2: PKB phosphorylation-dependent association of $FOXO4_{11-213}$ with 14-3-3ζ. Analytical gel filtration experiments were performed at a flow rate of 50 μL/min on a Pharmacia SmartSystem Superdex 75 column in 20 mM Tris (pH 7.5), 100 mM NaCl, 1 mM EDTA, 1 mM DTT buffer equilibrated at 4 °C. Samples (50 μL) contained 30 μM $FOXO4_{11-213}$ (A), 60 μM 14-3-3ζ (B), or a mixture of the two proteins (C, D). Fractions (50 μL each) were analyzed using 4−12% NuPAGE (Invitrogen) electrophoresis. Separated proteins were stained by Coomassie Blue, as shown in the inset gels with lane numbers corresponding to the time at which the fractions were collected.

Table 1: Summary of Sedimentation Equilibrium Experiments[a]

complex	K (M^{-1})	K_D (μM)
$dpFOXO4_{11-213}$ (WT) + $(14\text{-}3\text{-}3\zeta)_2$	3.3×10^{7} [b]	≤0.03[b]
$pFOXO4_{11-213}$ (T28A) + $(14\text{-}3\text{-}3\zeta)_2$	3.4×10^{6}	0.29
$FOXO4_{11-213}$ (T28A) + $(14\text{-}3\text{-}3\zeta)_2$	1.1×10^{5}	9
$pFOXO4_{11-213}$ (S193A) + $(14\text{-}3\text{-}3\zeta)_2$	1.5×10^{6}	0.65
$FOXO4_{11-213}$ (S193A) + $(14\text{-}3\text{-}3\zeta)_2$	1.9×10^{5}	5.3
$dpFOXO4_{11-213}$ + hIRE	2×10^{6}	0.5 ± 0.2
$pFOXO4_{11-213}$ (T28A) + hIRE	5×10^{6}	0.2 ± 0.1
$pFOXO4_{11-213}$ (S193A) + hIRE	2.2×10^{6}	0.45 ± 0.35

[a] Sedimentation equilibrium experiments of the $pFOXO4_{11-213}$:14-3-3ζ complexes were conducted at loading concentrations of 10−17 μM. Experiments to determine the stoichiometry of the $pFOXO4_{11-213}$:hIRE complexes were carried out at loading concentrations of 17−20 μM, whereas experiments to estimate the binding affinity of $pFOXO4_{11-213}$ for hIRE were carried out at 1/10 these loading concentrations. Samples were dialyzed against 20 mM Tris−HCl (pH 7.5), 100 mM NaCl, 1 mM EDTA, 2 mM 2-mercaptoethanol buffer prior to analysis. [b] Estimated value based on the loading concentration of the complex (see the text).

20770 ± 260 Da. So as not to introduce any bias based on differences in the partial specific volumes of the components, it is customary to use the buoyant molecular mass (i.e., $M(1 - \upsilon\rho)$, where M is the mass of the protein, υ is its partial specific volume, and ρ is the density of the solvent) to determine the stoichiometry of mixed component complexes. On the basis of the amino acid sequences of FOXO4 and 14-3-3ζ, buoyant molecular masses of 5955 and 7379 Da were calculated, respectively. Therefore, the dpFOXO4:14-3-3ζ complex with a 1:2 molar stoichiometry has a calculated buoyant molecular mass of 20712 Da. This value is consistent with that determined experimentally, within the error of the measurement, thereby establishing that one molecule of dpFOXO4 binds one dimer of 14-3-3ζ. The estimate of the molecular mass of the complex from the sedimentation equilibrium data assuming the 1:2 stoichiometry is 78250 ± 1000 Da, consistent with the mass of its components. We observed essentially complete complex formation between $dpFOXO4_{11-213}$ and 14-3-3ζ (i.e., at least 95% of FOXO4 and 14-3-3 was bound in the complex). Since the loading complex concentration was 10 μM, this allows us to conclude that the dissociation constant K_D for complex formation must be less than 30 nM.

The ability of the two 14-3-3 binding motifs to promote association of $FOXO4_{11-213}$ with 14-3-3 independently was tested by sedimentation equilibrium measurements using samples containing 14-3-3ζ and either of the phosphorylated

point mutants, pFOXO4$_{11-213}$ T28A or S193A. In both cases, incomplete complex formation, again with 1:2 molar stoichiometry, was noted. Noting that 14-3-3ζ has been shown to be dimeric in solution (*3*), data were modeled in terms of a reversible FOXO4 + (14-3-3ζ)$_2$ ↔ FOXO4:(14-3-3ζ)$_2$ equilibrium to yield dissociation constants K_D of 0.29 μM for pFOXO4$_{11-213}$ T28A:(14-3-3ζ)$_2$ and 0.65 μM for pFOXO4$_{11-213}$ S193A:(14-3-3ζ)$_2$ (Table 1). These results demonstrate that while singly phosphorylated FOXO4 mutants containing only one 14-3-3 binding motif can bind to 14-3-3ζ, the binding affinity is at least an order of magnitude weaker than that of the doubly phosphorylated FOXO4.

Association with 14-3-3 Inhibits FOXO4$_{11-213}$ DNA Binding. FOXO transcription factors activate gene transcription through binding to the AAACA-motif-containing insulin response element (IRE) (*31*, *32*). In the case of the *C. elegans* homologue DAF-16, it has been demonstrated that 14-3-3 binding induced by PKB phosphorylation inhibits DAF-16 binding to DNA (*10*). This suggests that association of FOXO proteins (or DAF-16) with 14-3-3 can be the first step in the process of release of FOXO factors from DNA. When dpFOXO4$_{11-213}$ was mixed with an equimolar amount of dsDNA representing part of the insulin response element (hIRE), analytical gel filtration experiments demonstrated that hIRE comigrated with dpFOXO4$_{11-213}$ (Figure 3A−C), on the basis of the ratio of the absorptions at 280 and 260 nm. The same result was obtained for unphosphorylated FOXO4$_{11-213}$ (data not shown), indicating that PKB phosphorylation itself does not affect FOXO4 DNA binding. However, in the presence of 14-3-3ζ at twice the molar ratio of dpFOXO4$_{11-213}$, no DNA comigrated with the protein−protein complex (Figure 3D−E). This result was not dependent on the order of addition of the various components.

Electrophoretic mobility shift assays were used to confirm the results obtained by gel filtration. As shown in Figure 4, phosphorylation of FOXO4$_{11-213}$ by PKB did not affect its DNA binding (Figure 4A,B). However, in the presence of 14-3-3ζ, dpFOXO4$_{11-213}$ does not bind detectably to hIRE (Figure 4A; compare lanes 5 and 7). This 14-3-3-dependent inhibition of dsDNA binding requires phosphorylated FOXO4; unphosphorylated FOXO4$_{11-213}$ can still bind hIRE in the presence of 14-3-3ζ (Figure 4A,B; compare lanes 7 and 8), indicating that a complex of phosphorylated FOXO4$_{11-213}$ and 14-3-3ζ is needed for efficient inhibition of IRE binding.

Efficient 14-3-3-Dependent Inhibition of FOXO4$_{11-213}$ DNA Binding Requires Two 14-3-3 Binding Motifs. To further characterize the link between PKB phosphorylation of FOXO4 and 14-3-3-dependent inhibition of DNA binding, we tested the DNA binding properties of singly phosphorylated FOXO4 mutants in the presence of 14-3-3ζ. First, the stoichiometries of the FOXO4:hIRE complexes and the binding affinities of dpFOXO4$_{11-213}$, pFOXO4$_{11-213}$ T28A, and pFOXO4$_{11-213}$ S193A for hIRE were determined by sedimentation equilibrium. Complex stoichiometries and hIRE buoyant molecular masses were determined at high loading concentrations. The hIRE was monodisperse and double-stranded under these conditions, and all three FOXO4:hIRE mixtures were monodisperse. In all cases, buoyant molecular masses correspond (within the error of the method) to masses calculated on the basis of the experimental hIRE buoyant mass for 1:1 FOXO4:hIRE complexes ($n = 1.1$). Dissociation constants were determined at lower sample loading concentrations, and data were analyzed in terms of a reversible FOXO4 + hIRE ↔ FOXO4:hIRE equilibrium to yield dissociation constants of 0.5 ± 0.2 μM (dpFOXO4$_{11-213}$), 0.2 ± 0.1 μM (pFOXO4$_{11-213}$ T28A), and 0.45 ± 0.35 μM (pFOXO4$_{11-213}$ S193A). All data fits were good, and we conclude that, within the error of the method, the affinities of the wild-type, T28A, and S193A pFOXO4$_{11-213}$ proteins for hIRE are identical.

Experiments with dpFOXO4$_{11-213}$ showed that 14-3-3ζ binding efficiently inhibits FOXO4 DNA binding. To elucidate whether double phosphorylation of FOXO4$_{11-213}$ is necessary for complete 14-3-3-dependent inhibition of DNA binding, we performed sedimentation equilibrium experiments with 14-3-3 complexes of dpFOXO4$_{11-213}$ or singly phosphorylated FOXO4$_{11-213}$ mutants in the presence of hIRE. Data obtained for a mixture of 14-3-3ζ, dpFOXO4$_{11-213}$, and hIRE (Figure 5A,B) were best modeled in terms of a mixture of free hIRE and a complex whose mass corresponds to that of a dpFOXO4$_{11-213}$:14-3-3ζ (1:2) complex. A poor fit was obtained when the data were analyzed in terms of a mixture of the 14-3-3ζ dimer and a dpFOXO4$_{11-213}$:hIRE complex, indicating that this model is inappropriate (Figure 5C). On the basis of the experimentally determined weight-average buoyant molecular masses, it seems that the same holds true for samples containing singly phosphorylated FOXO4$_{11-213}$ mutants. However, in these cases, incomplete pFOXO4$_{11-213}$:14-3-3ζ complex formation was observed, indicating that a portion of pFOXO4$_{11-213}$ is not bound to a 14-3-3 dimer. These results were confirmed by electrophoretic mobility shift assays, which clearly showed that pFOXO4$_{11-213}$:hIRE complexes can be formed in the presence of 14-3-3ζ (Figure 4A,B; compare lanes 7, 9, and 10), likely because singly phosphorylated pFOXO4$_{11-213}$ mutants have similar binding affinities for 14-3-3ζ and hIRE (Table 1). Therefore, the presence of two 14-3-3 binding motifs is required for high-affinity association of FOXO4$_{11-213}$ with 14-3-3ζ and efficient inhibition of DNA binding. A model consistent with these results is shown in Figure 6.

DISCUSSION

14-3-3 isoforms form very stable homo- and heterodimers containing two ligand binding grooves oriented in opposite directions (*1*, *3*, *13*, *14*). A ligand containing two 14-3-3 binding motifs can therefore bind to a 14-3-3 dimer employing both motifs, and several well-characterized 14-3-3 binding partners contain at least two 14-3-3 binding motifs (*1*, *3*, *10*). It therefore has been speculated that interactions between the 14-3-3 dimer and a ligand containing two 14-3-3 binding sites could stabilize binding and localize the binding partner in the central channel of the 14-3-3 dimer more effectively than binding using only one binding motif. This would allow for a wider or more varied range of biological function based on differential phosphorylation. This notion becomes even more attractive if one considers the fact that 14-3-3 proteins are capable of binding a large number of different partners that, with the exception of the short binding motifs, lack sequence and presumably structural homology.

The first structural insights into the binding of a fully active target protein by 14-3-3 were provided by the crystal structure of the serotonin *N*-acetyltransferase (AANAT):14-3-3ζ complex (*3*). Formation of this complex is absolutely

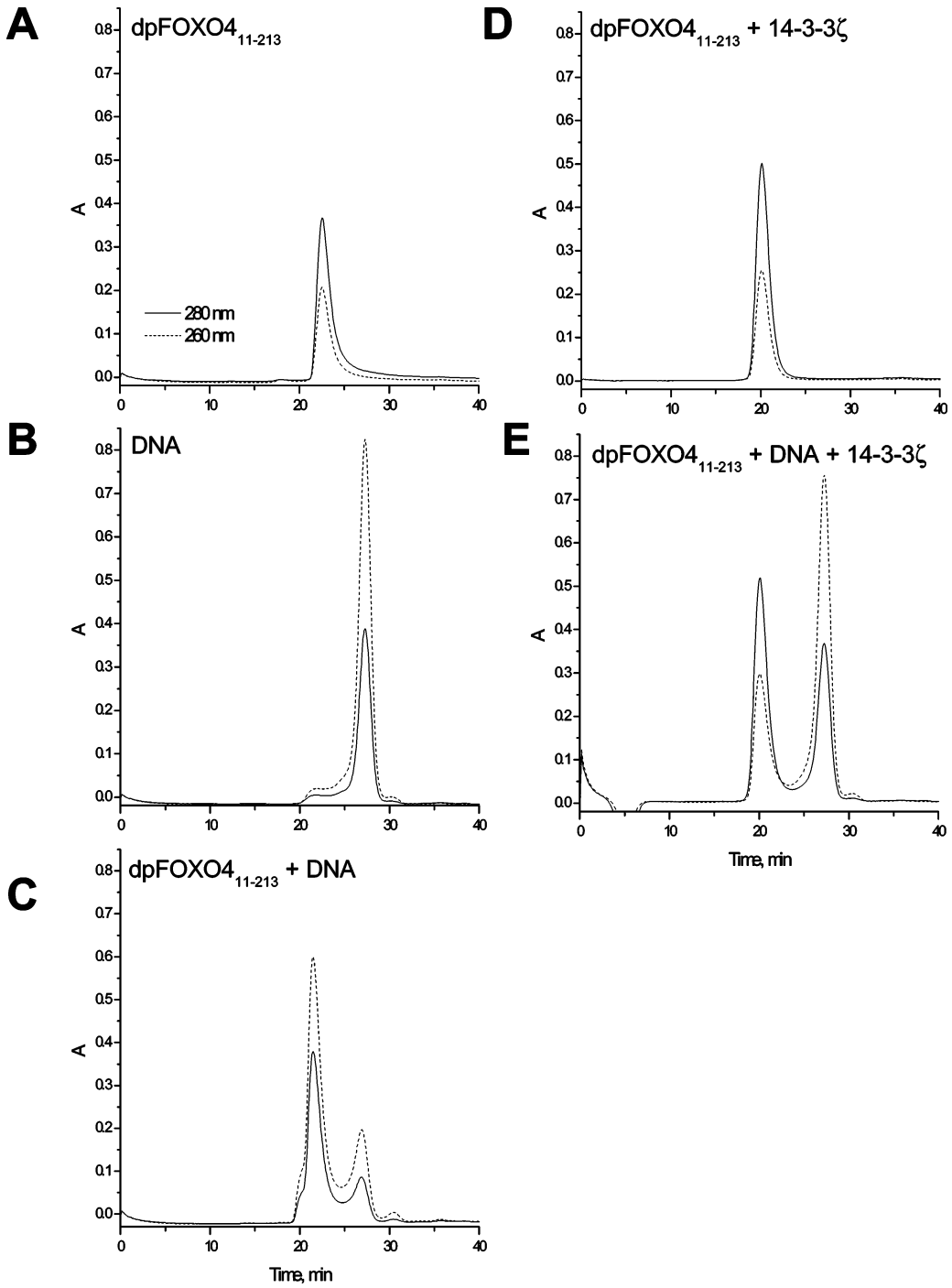

FIGURE 3: 14-3-3ζ binding inhibits dpFOXO4$_{11-213}$ DNA binding. Analytical gel filtration experiments were performed at a flow rate of 50 μL/min on a Pharmacia SmartSystem Superdex 75 column in 20 mM Tris (pH 7.5), 100 mM NaCl, 1 mM EDTA, 1 mM DTT buffer equilibrated at 4 °C. Samples (50 μL) contained combinations of 30 μM FOXO4$_{11-213}$, 30 μM DNA (hIRE, top strand 5′-GCAAAACAAA-3′), and 60 μM 14-3-3ζ as indicated.

dependent on phosphorylation of Thr-31, a protein kinase A (PKA) substrate. To obtain diffracting crystals, it was necessary to use a slightly truncated version of the enzyme in which the last six C-terminal residues were deleted. This region included Ser-205, a substrate of PKA that is also phosphorylated (*33*). The crystal structure showed that two molecules of singly phosphorylated truncated AANAT, pAANAT$_{1-201}$, each containing one 14-3-3 binding motif centered on pThr-31, are bound in the central channel of the 14-3-3 dimer, forming a complex with 2:2 stoichiometry. In this complex, pAANAT$_{1-201}$ interacts with 14-3-3 through extensive contacts with both the amphipathic binding grooves and other regions of the central channel. The two 14-3-3 binding motifs of pAANAT$_{1-201}$, centered on the pT31 residues, each occupy one of the amphipathic binding grooves of a 14-3-3 monomer. Interactions between the two molecules that are distinct from the ones involving the binding motif stabilize AANAT in a conformation that enhances its catalytic competence and provides a functional explanation for the interaction. Molecular modeling indicated that if the deleted C-terminal region was present and Ser-205 was phosphorylated, the additional six amino acids could interfere with the interaction that the N-terminus of the other pAANAT$_{1-201}$ molecule forms with 14-3-3 (*3*). Correspondingly, sedimen-

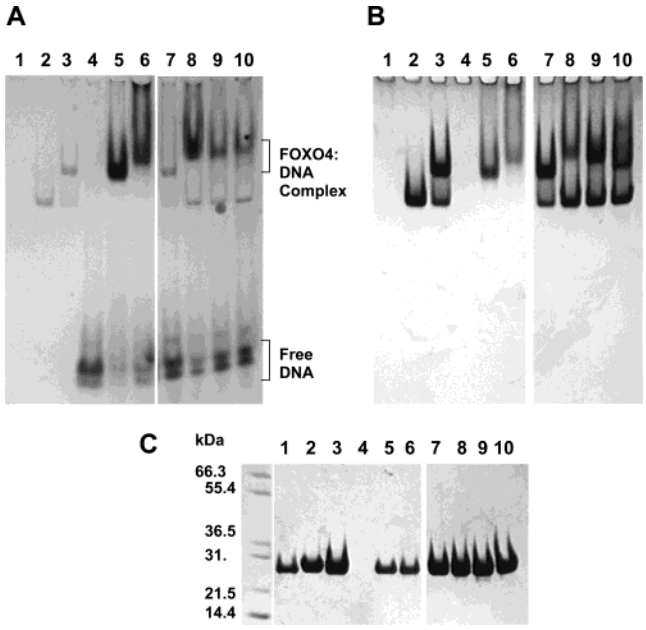

FIGURE 4: Efficient 14-3-3-dependent inhibition of dpFOXO4$_{11-213}$ DNA binding requires two 14-3-3 binding motifs. (A) Native 4−20% TBE−PAGE electrophoresis, silver staining for hIRE. (B) Native 4−20% TBE−PAGE electrophoresis, Coomassie Blue staining. (C) 4−12% NuPAGE electrophoresis, Coomassie Blue staining. Key: lane 1, dpFOXO4$_{11-213}$; lane 2, 14-3-3ζ; lane 3, dpFOXO4$_{11-213}$:14-3-3ζ dimer (molar stoichiometry 1:1) complex; lane 4, hIRE (sequence 5′-GCAAAACAAA-3′); lane 5, dpFOXO4$_{11-213}$:hIRE (molar stoichiometry 1:1) complex; lane 6, FOXO4$_{11-213}$:hIRE (molar stoichiometry 1:1) complex; lane 7, dpFOXO4$_{11-213}$:hIRE:14-3-3ζ dimer (molar stoichiometry 1:1:1); lane 8, FOXO4$_{11-213}$:hIRE:14-3-3ζ dimer (molar stoichiometry 1:1:1) complex; lane 9, pFOXO4$_{11-213}$ (Thr28Ala):hIRE:14-3-3ζ dimer (molar stoichiometry 1:1:1) complex; lane 10, pFOXO4$_{11-213}$ (Ser193Ala):hIRE:14-3-3ζ dimer (molar stoichiometry 1:1:1) complex.

tation equilibrium measurements indicated that while pAANAT$_{1-201}$ can form 2:2 complexes with 14-3-3, full-length doubly phosphorylated AANAT, dpAANAT$_{1-207}$, forms only 1:2 complexes, with a single enzyme molecule bound to the 14-3-3 dimer. Taken together, these observations suggest that the biologically relevant form of the AANAT:14-3-3ζ complex is that in which one molecule of AANAT is bound to 14-3-3 through two phosphorylation sites.

Similarly to AANAT, many other binding partners of 14-3-3 proteins contain multiple phosphorylation sites embedded in 14-3-3 recognition motifs (*16*). There are several possible interpretations of this observation. For example, it is possible that, under different conditions, different sites could be phosphorylated, and that—in principle—different complexes could form which would either expose or mask different parts of the binding partner. It is also possible that two molecules of the binding partner could bind to a single dimer of 14-3-3; alternatively, two different binding partners could bind to a single 14-3-3 dimer. On the other hand, in cases when a single kinase can phosphorylate multiple 14-3-3 binding sites on a single binding partner, it is more likely that, as for AANAT, two of these sites within a single molecule would be used at the same time. Having two "anchors" would increase the stability of the complex, as has been demonstrated in a model polypeptide system. When two phosphorylated motifs were present, the peptide bound to 14-3-3 with much higher affinity ($K_D \approx 20$ nM) compared with the same peptide in which only one of the two motifs was phosphorylated ($K_D \approx 730$ nM) (*15*). This effect was also seen when the stability of the pAANAT$_{1-201}$:14-3-3ζ complex was compared to that of dpAANAT$_{1-207}$:14-3-3ζ, in which it was observed that the doubly phosphorylated binding partner formed complexes that were substantially more stable.[2]

Similarly to AANAT, PKB-mediated phosphorylation of FOXO transcription factors creates multiple 14-3-3 binding sites. This results in nuclear exit, cytoplasmic retention, and inactivation of FOXO transcriptional activity (*8*, *9*). However, details of interactions between 14-3-3 and FOXO4 remain unclear. To obtain insight into the mechanism of 14-3-3-dependent FOXO4 regulation, we have biophysically characterized the interactions among 14-3-3ζ, FOXO4, and DNA representing part of the IRE. Since FOXO4's close homologues FOXO1 and FOXO3a bind to 14-3-3 through motifs created by the phosphorylation of the P1 site and P1 + P2 sites, respectively, we expressed and purified the N-terminal half of FOXO4 containing the DNA binding domain and two PKB phosphorylation/14-3-3 binding sites, P1 and P2 (Figure 1). We have shown that (i) incubation of PKB with FOXO4$_{11-213}$ in vitro leads to complete phosphorylation of both Thr-28 and Ser-193, (ii) upon PKB-mediated phosphorylation, both these sites are binding motifs for 14-3-3ζ, (iii) doubly phosphorylated dpFOXO4$_{11-213}$ binds 14-3-3ζ with significantly higher affinity than singly phosphorylated mutants, and (iv) double phosphorylation of FOXO4$_{11-213}$ and the associated high-affinity association with 14-3-3ζ are required for efficient competition with DNA binding.

Data describing PKB phosphorylation of FOXO4 at Thr-28 (P1 site), as well as functional consequences of this phosphorylation, are controversial. It has been reported that Thr-28 is phosphorylated and required for FOXO4 nuclear export in CHO cells (*21*), but not in NIH 3T3 cells (*26*). Our data demonstrate that PKB phosphorylates FOXO4$_{11-213}$ in vitro completely at both Thr-28 and Ser-193 (Table 1). This is consistent with the well-established PKB phosphorylation of the corresponding site in FOXO1 (Thr-24) and FOXO3a (Thr-32) (*8*, *34*).

Recently, Zhang et al. reported that mutation of FOXO1 Ser-256 (P2 site) to aspartate, which mimics the effect of phosphorylation, alters DNA binding affinity from 93 ± 9 to 263 ± 24 nM (*35*). However, we did not observe any significant effect of PKB phosphorylation on the affinity of FOXO4 for hIRE. This result is consistent with data obtained for the *C. elegans* FOXO homologue, DAF-16, where it has been shown that phosphorylation alone does not affect DNA binding (*10*). Our gel shift, gel filtration, and sedimentation equilibrium experiments revealed essentially the same DNA binding affinity for unphosphorylated, doubly phosphorylated, and singly phosphorylated FOXO4$_{11-213}$. Observed FOXO4$_{11-213}$ DNA binding affinities (0.2−0.5 μM) are in the same range as reported FOXO1 DNA binding affinities. The slightly higher binding affinity reported in the case of FOXO1 might reflect true differences in the truncated proteins used (residues 160−266 of FOXO1 in ref *35* versus residues 11−213 of FOXO4), or the slightly higher ionic strength used in the experiments described here.

To date, several structures of different Forkhead DNA binding domains have been determined from, for example,

[2] T.O. Unpublished observations.

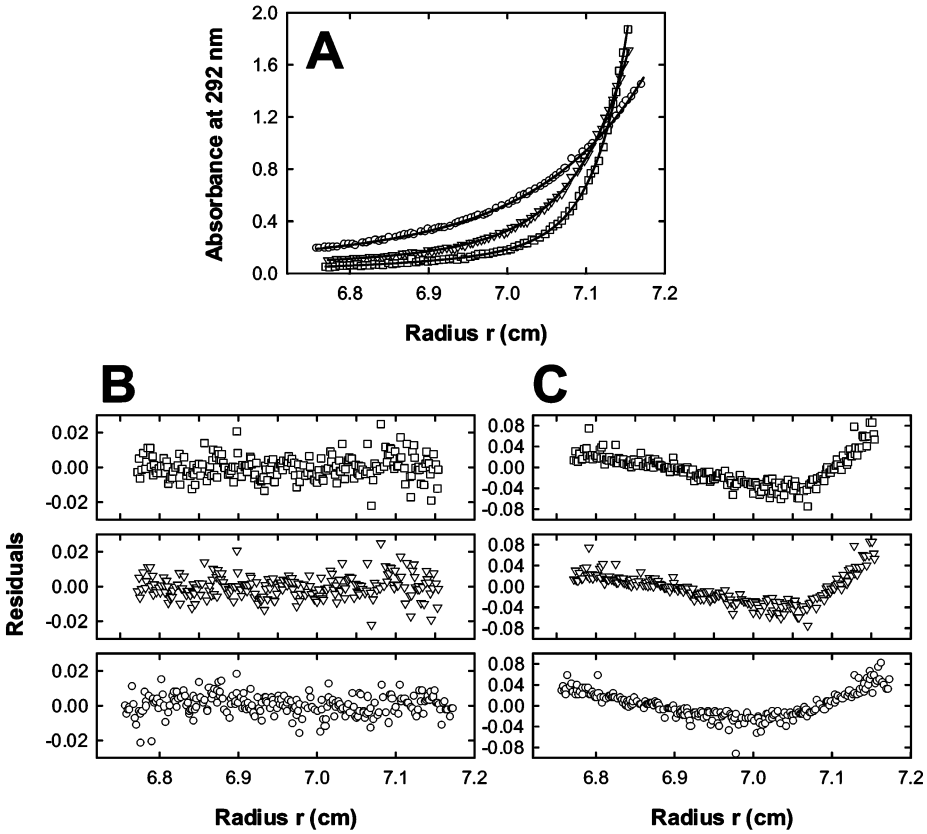

FIGURE 5: Efficient 14-3-3-dependent inhibition of dpFOXO4$_{11-213}$ DNA binding. (A) Sedimentation equilibrium profiles at 292 nm and 4.0 °C for a 1:1:1 mixture of dpFOXO4$_{11-213}$, hIRE, and 14-3-3ζ dimer (17.2 μM each). Symbols correspond to data collected at 10000 (circles), 14000 (triangles), and 18000 (squares) rpm. For clarity, only one in three data points are shown. The full data complement is represented in the residual plots. (B) Data analysis in terms of two noninteracting ideal solutes is consistent with a dpFOXO4$_{11-213}$:(14-3-3ζ)$_2$ complex and free hIRE. The lines through the data in (A) represent this best fit analysis. Residuals corresponding to the best fit analysis in terms of two ideal solutes are shown. (C) A poor fit for data analysis in terms of the presence of a dpFOXO4$_{11-213}$:hIRE complex and free (14-3-3ζ)$_2$ is evidenced by the corresponding residuals. Similar observations were made when the experiments were carried out at loading concentrations of 1.7 μM.

HNF-3γ (*36*), transcription factor Genesis (*37*), and FOXO4 (*27*). Two of them, HNF-3γ and Genesis, were also solved in complex with DNA. All structures are similar, revealing a typical Forkhead winged-helix fold where three α-helices are tightly packed against each other with two small antiparallel β-strands containing two loops ("wings"). These proteins interact with DNA as monomers in which the main contact interface is provided by one of three α-helices, which lies in the major groove of DNA. The PKB phosphorylation site P2 (i.e., Ser-193 of FOXO4) and a nearby nuclear localization sequence are in close proximity to the FOXO DNA binding domain. Therefore, in theory, phosphorylation-mediated 14-3-3 binding could sterically interfere with the function of the DNA binding domain, the NLS, or both. Our observation that FOXO4$_{11-213}$ needs two 14-3-3 binding motifs for high-affinity association with 14-3-3ζ and efficient inhibition of DNA binding suggests that another mechanism, e.g., a conformational change of the DNA binding domain, could be involved, as shown in the model in Figure 6. The need for two phosphorylation/14-3-3 binding sites to achieve efficient DNA binding inhibition was also reported for the 14-3-3-dependent inhibition of DAF-16 DNA binding. In this case, concurrent PKB phosphorylation of DAF-16 at residues Thr-54 (site P1) and Ser-314 (site P3) triggers 14-3-3 binding and inhibition of DNA binding (*10*). We note that two phosphorylation sites which serve as 14-3-3 recognition motifs flanking a DNA binding domain lead to a model for FOXO4:14-3-3ζ complex formation in which the Forkhead domain is sequestered in the central channel of the 14-3-3 dimer, a mode of binding that would be similar to that observed for AANAT bound to 14-3-3 (*3*). Such a mode of binding is consistent with the gel filtration results shown in Figure 2, in which the dpFOXO4$_{11-213}$:14-3-3ζ complex elutes at essentially the same position as 14-3-3ζ alone (compare parts B and C of Figure 2), as would be expected if the hydrodynamic radii were similar in both cases.

Our data provide a quantitative framework to understand how multiple, competing associations can achieve the desired regulatory effect even though each of the separate complexes can form with high affinity (Figure 6). Although FOXO4 can bind the IRE-containing DNA with a K_D of 400 nM, if PKB is activated and FOXO4 becomes phosphorylated at the two 14-3-3 binding motifs, the stronger association with 14-3-3 (K_D of less than 30 nM) and the lack of measurable ability of the resulting FOXO4:14-3-3 complex to bind DNA will give rise to an equilibrium where most of the FOXO4 is dissociated from the DNA. Subsequent nuclear export of the complex (*9*) will complete the process. The data presented in this work strongly suggest that, for this to happen, FOXO4 must be phosphorylated at both P1 and P2 sites. Furthermore, the requirement of concurrent phosphorylation of two sites for high-affinity 14-3-3 binding could explain the prevalence of multiple phosphorylation and 14-3-3 binding sites not only

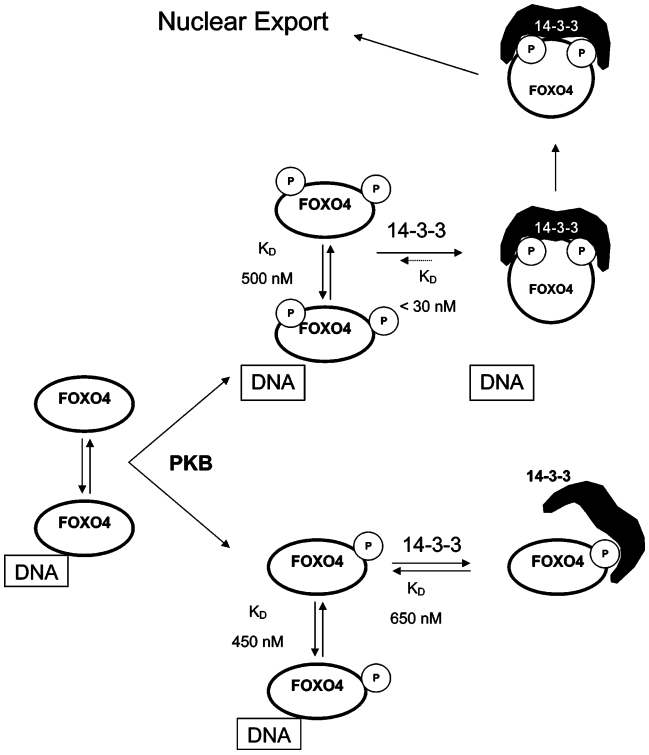

FIGURE 6: Effect of PKB phosphorylation and 14-3-3 binding on FOXO4 DNA binding. PKB phosphorylation of FOXO4 creates two 14-3-3 binding sites, while phosphorylation itself does not affect DNA binding affinity. FOXO4 containing two 14-3-3 binding sites interacts tightly with a 14-3-3 dimer (top pathway). Since the binding affinity of FOXO4 for 14-3-3 is an order of magnitude higher than that for DNA, all FOXO4 is bound in the complex with 14-3-3 and DNA binding is completely inhibited. However, if partial phosphorylation of FOXO4 generates only one 14-3-3 binding site (bottom pathway), the resulting FOXO4:14-3-3 complex cannot effectively compete with DNA binding (indicated binding affinities of singly phosphorylated FOXO4 are those obtained for the S193A mutant). Moreover, interactions between 14-3-3 and FOXO4 through two 14-3-3 binding sites could induce a conformational change needed for DNA binding inhibition, and which could not be achieved in the absence of one of the 14-3-3 binding sites.

in the case of FOXO4 and other FOXO homologues, but also with other 14-3-3 binding partners.

Finally, it is worth noting the range of measured binding constants for the interaction of 14-3-3ζ with unphosphorylated, singly phosphorylated, and doubly phosphorylated $FOXO4_{11-213}$ (shown in Table 1). While $dpFOXO4_{11-213}$:14-3-3ζ is clearly a stable complex, with a K_D of less than 30 nM, all other $FOXO4_{11-213}$ (either phosphorylated or not) combinations interact with 14-3-3ζ to a measurable degree. This range of binding constants may provide an explanation for apparent discrepancies when qualitative techniques such as yeast two-hybrid or pull-down assays are used to characterize macromolecular interactions where the threshold for complex detection is not known. Quantitative techniques, such as sedimentation equilibrium, provide a clear advantage when complex systems are analyzed.

REFERENCES

1. Fu, H., Subramanian, R. R., and Masters, S. C. (2000) *Annu. Rev. Pharmacol. Toxicol. 40*, 617−647.
2. Banik, U., Wang, G. A., Wagner, P. D., and Kaufman, S. (1997) *J. Biol. Chem. 272*, 26219−26225.
3. Obsil, T., Ghirlando, R., Klein, D. C., Ganguly, S., and Dyda, F. (2001) *Cell 105*, 257−267.
4. Muslin, A. J., and Xing, H. (2000) *Cell Signal 12*, 703−709.
5. Lopez-Girona, A., Furnari, B., Mondesert, O., and Russell, P. (1999) *Nature 397*, 172−175.
6. Seimiya, H., Sawada, H., Muramatsu, Y., Shimizu, M., Ohko, K., Yamane, K., and Tsuruo, T. (2000) *EMBO J. 19*, 2652−2661.
7. Grozinger, C. M., and Schreiber, S. L. (2000) *Proc. Natl. Acad. Sci. U.S.A. 97*, 7835−7840.
8. Brunet, A., Bonni, A., Zigmond, M. J., Lin, M. Z., Juo, P., Hu, L. S., Anderson, M. J., Arden, K. C., Blenis, J., and Greenberg, M. E. (1999) *Cell 96*, 857−868.
9. Brunet, A., Kanai, F., Stehn, J., Xu, J., Sarbassova, D., Frangioni, J. V., Dalal, S. N., DeCaprio, J. A., Greenberg, M. E., and Yaffe, M. B. (2002) *J. Cell. Biol. 156*, 817−828.
10. Cahill, C. M., Tzivion, G., Nasrin, N., Ogg, S., Dore, J., Ruvkun, G., and Alexander-Bridges, M. (2001) *J. Biol. Chem. 276*, 13402−13410.
11. Rittinger, K., Budman, J., Xu, J., Volinia, S., Cantley, L. C., Smerdon, S. J., Gamblin, S. J., and Yaffe, M. B. (1999) *Mol. Cell 4*, 153−166.
12. Aitken, A. (1996) *Trends Cell. Biol. 6*, 341−347.
13. Yaffe, M. B., Rittinger, K., Volinia, S., Caron, P. R., Aitken, A., Leffers, H., Gamblin, S. J., Smerdon, S. J., and Cantley, L. C. (1997) *Cell 91*, 961−971.
14. Xiao, B., Smerdon, S. J., Jones, D. H., Dodson, G. G., Soneji, Y., Aitken, A., and Gamblin, S. J. (1995) *Nature 376*, 188−191.
15. Liu, D., Bienkowska, J., Petosa, C., Collier, R. J., Fu, H., and Liddington, R. (1995) *Nature 376*, 191−194.
16. Yaffe, M. B. (2002) *FEBS Lett. 513*, 53−57.
17. Burgering, B. M., and Kops, G. J. (2002) *Trends Biochem. Sci. 27*, 352−360.
18. So, C. W., and Cleary, M. L. (2002) *Mol. Cell. Biol. 22*, 6542−6552.
19. Medema, R. H., Kops, G. J., Bos, J. L., and Burgering, B. M. (2000) *Nature 404*, 782−787.
20. Paradis, S., and Ruvkun, G. (1998) *Genes Dev. 12*, 2488−2498.
21. Rena, G., Woods, Y. L., Prescott, A. R., Peggie, M., Unterman, T. G., Williams, M. R., and Cohen, P. (2002) *EMBO J. 21*, 2263−2271.
22. Woods, Y. L., Rena, G., Morrice, N., Barthel, A., Becker, W., Guo, S., Unterman, T. G., and Cohen, P. (2001) *Biochem. J.* 355, 597−607.
23. Rena, G., Prescott, A. R., Guo, S., Cohen, P., and Unterman, T. G. (2001) *Biochem. J. 354*, 605−612.
24. Takaishi, H., Konishi, H., Matsuzaki, H., Ono, Y., Shirai, Y., Saito, N., Kitamura, T., Ogawa, W., Kasuga, M., Kikkawa, U., and Nishizuka, Y. (1999) *Proc. Natl. Acad. Sci. U.S.A. 96*, 11836−11841.
25. Brownawell, A. M., Kops, G. J., Macara, I. G., and Burgering, B. M. (2001) *Mol. Cell. Biol. 21*, 3534−3546.
26. Kops, G. J. P. L., de Ruiter, N. D., De Vries-Smits, A. M. M., Powell, D. R., Bos, J. L., and Burgering, B. M. T. (1999) *Nature 398*, 630−634.
27. Weigelt, J., Climent, I., Dahlman-Wright, K., and Wikstrom, M. (2001) *Biochemistry 40*, 5861−5869.
28. Ghirlando, R., Keown, M. B., Mackay, G. A., Lewis, M. S., Unkeless, J. C., and Gould, H. J. (1995) *Biochemistry 34*, 13320−13327.
29. Palfner, K., Kneba, M., Hiddemann, W., and Bertram, J. (1995) *Biotechniques 19*, 926−929.
30. Jacobs, F. M., Van Der Heide, L. P., Wijchers, P. J., Burbach, J. P., Hoekman, M. F., and Smidt, M. P. (2003) *J. Biol. Chem. 278*, 35959−35967.
31. Furuyama, T., Nakazawa, T., Nakano, I., and Mori, N. (2000) *Biochem. J. 349*, 629−634.
32. Biggs, W. H. 3rd, Cavenee, W. K., and Arden, K. C. (2001) *Mamm. Genome 12*, 416−425.
33. Klein, D. C., Ganguly, S., Coon, S. L., Shi, Q., Gaildret, P., Morin, F., Weller, J. L., Obsil, T., Hickman, A. B., and Dyda, F. (2003) *J. Neuroendocrinol. 15*, 370−377.
34. Woods, Y. L., and Rena, G. (2002) *Biochem. Soc. Trans. 30*, 391−397.
35. Zhang, X. H., Gan, L., Pan, H. Y., Guo, S. D., He, X. W., Olson, S. T., Mesecar, A., Adam, S., and Unterman, T. G. (2002) *J. Biol. Chem. 277*, 45276−45284.
36. Clark, K. L., Halay, E. D., Lai, E., and Burley, S. K. (1993) *Nature 364*, 412−420.
37. Jin, C., Marsden, I., Chen, X., and Liao, X. (1999) *J. Mol. Biol. 289*, 683−690.

BI0352724